Materials
Views
www.MaterialsViews.com

ADVANCED
FUNCTIONAL
MATERIALS
www.afm-journal.de

FULL PAPER

Genetically Engineered Phage Fibers and Coatings for Antibacterial Applications

By *Joan Y. Mao, Angela M. Belcher,* and *Krystyn J. Van Vliet**

Multifunctionality can be imparted to protein-based fibers and coatings via either synthetic or biological approaches. Here, potent antimicrobial functionality of genetically engineered, phage-based fibers and fiber coatings, processed at room temperature, is demonstrated. Facile genetic engineering of the M13 virus (bacteriophage) genome leverages the well-known antibacterial properties of silver ions to kill bacteria. Predominant expression of negatively charged glutamic acid (E3) peptides on the pVIII major coat proteins of M13 bacteriophage enables solution-based, electrostatic binding of silver ions and subsequent reduction to metallic silver along the virus length. Antibacterial fibers of micrometer-scale diameters are constructed from such an E3-modified phage via wet-spinning and glutaraldehyde-crosslinking of the E3-modified viruses. Silverization of the free-standing fibers is confirmed via energy dispersive spectroscopy and inductively coupled plasma atomic emission spectroscopy, showing $\sim$0.61 μg cm^{-1} of silver on E3–Ag fibers. This degree of silverization is threefold greater than that attainable for the unmodified M13–Ag fibers. Conferred bactericidal functionality is determined via live–dead staining and a modified disk-diffusion (Kirby–Bauer) measure of zone of inhibition (ZoI) against *Staphylococcus epidermidis* and *Escherichia coli* bacterial strains. Live–dead staining and ZoI distance measurements indicate increased bactericidal activity in the genetically engineered, silverized phage fibers. Coating of Kevlar fibers with silverized E3 phage exhibits antibacterial effects as well, with relatively smaller ZoIs attributable to the lower degree of silver loading attainable in these coatings. Such antimicrobial functionality is amenable to rapid incorporation within fiber-based textiles to reduce risks of infection, biofilm formation, or odor-based detection, with the potential to exploit the additional electronic and thermal conductivity of fully silverized phage fibers and coatings.

1. Introduction

Materials containing silver ions and compounds are well known to exhibit strong antibacterial functionality against a broad spectrum of bacterial strains.[1] The antibacterial mode of action involves Ag$^+$ coordination to electron-donating functional groups, such as the thiols found on the membranes of bacteria cells, consequently disturbing membrane permeability and leading to cell death.[2,3] Such a mechanism renders bacteria unlikely to develop a resistance to silver-based antimicrobial agents, and silver has a relatively low toxicity to mammalian cells.[4] For these reasons, scientists have incorporated metallic or ionic silver into a wide variety of platforms including silica glass,[5] nanoparticles,[6] polyelectrolyte multilayers,[7] nanofibers,[8] and various polymers[9–11] for consumer and industrial applications. Over the past decade, numerous efforts have been directed at producing textile fibers and coatings with antimicrobial capabilities.[8,11,12–14] Antibacterial fibers have application in the biomedical, water filtration, clothing, and healthcare industries. The vast majority of such antimicrobial fibers involve polymers in some capacity, either woven into another textile or assembled as nonwoven mats. Often, natural or synthetic polymers are grafted or chemically conjugated to antimicrobial agents such as antibiotics,[15] quaternary ammonium moieties,[16] phenols,[17] and halogenated compounds.[18] However, due to the reaction selectivity of the base polymer, additional or multiple functionalities can be difficult to impart upon such fibers.

Viruses require bacterial hosts for parasitic replication of the viral genome, but also present an intriguing and contradictory opportunity to engineer multifunctional, antibacterial fibers. Manipulation of the viral DNA enables the potential for multifunctionalization of the virus surface via controlled expression of different peptides on the outer capsid proteins of the virus coat. We have shown previously that genetically engineered virus fibers can be fabricated via wet-spinning through a solution of glutaraldehyde crosslinkers to bind gold.[19] Here, we modify and leverage this technology to create fibers and coatings useful for antibacterial applications. We present a novel method for creating bactericidal fibers by functionalizing a controllable, biological scaffold with silver particles. The building block comprising this scaffold is the
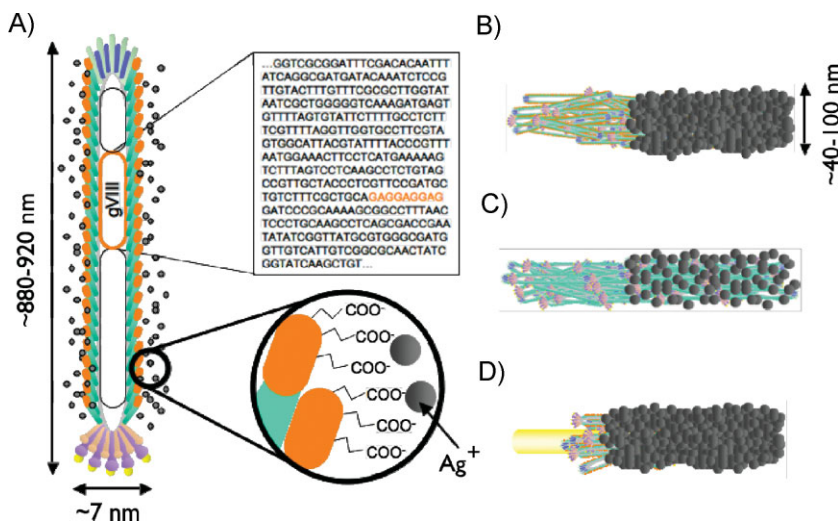
[*] Prof. A. M. Belcher, Prof. K. J. Van Vliet, J. Y. Mao
Department of Materials Science and Engineering
Department of Biological Engineering
Massachusetts Institute of Technology
8-237, 77 Massachusetts Ave., Cambridge, MA 02139 (USA)
E-mail: belcher@mit.edu; krystyn@mit.edu

ADVANCED
FUNCTIONAL
MATERIALS
www.afm-journal.de

Materials
Views
www.MaterialsViews.com

Figure 1. A) Schematic depiction of single M13 bacteriophage with DNA sequence engineered (gVIII, orange) to express three negatively charged glutamates on the body coat proteins (pVIII, orange ovals). This E3 sequence can electrostatically attract Ag$^+$. In this study, phage were glutaraldehyde-crosslinked upon extrusion to produce fibers comprising B) pVIII-altered E3 and C) wildtype M13 phage that attract Ag$^+$ to a lesser degree. D) Kevlar fibers were also coated with crosslinked E3 phage. On all fibers, bound Ag$^+$ were reduced to metallic particles in situ via sodium borohydride.

M13 filamentous bacteriophage (or virus, termed hereafter as phage); in biological contexts, these phage exclusively infect bacteria as opposed to mammalian cells. The M13 phage is a high-aspect-ratio phage with a length of approximately 880 nm and a diameter of 6–7 nm. Its capsid is composed of five modifiable proteins. Of these, the *gene VIII* major capsid protein (pVIII) comprises the main longitudinal length of the capsid; the phage displays about 2 700 copies of pVIII proteins. Functionalities of the M13 bacteriophage can be manipulated via molecular cloning into the single-stranded viral DNA genome to display peptides on the capsid proteins.[19–21]

Here, we aim to optimize the antibacterial properties of our phage-based fibers by employing a genetically engineered glutamate-rich phage (E3), shown in Figure 1A, which expresses three glutamate and one aspartate amino acid at the *N*-terminus of pVIII. This E3 motif includes one more negatively charged amino acid than the wildtype M13KE phage. Consequently, the surface of the phage presents an amplified negative charge, allowing for the functionalization of the phage with silver ions through nonspecific electrostatic interactions.[22] Subsequent reduction of the silver ions gives rise to a coating of silver particles along the body of the phage.[22] Continuous fibers of micrometer-scale diameter and centimeter-scale length were extruded via the extrusion method described by Chiang et al.[19] To explore the application of these crosslinked phage as coatings for fibers of relatively greater mechanical strength,[19] Kevlar fibers were coated with phage solution and crosslinked with glutaraldehyde. After crosslinking, both pure phage fibers and Kevlar composite fibers were plated with silver by electroless deposition using silver acetate as a silver ion precursor and subsequently reducing with sodium borohydride. This electroless deposition and reduction is referred to as silverization of the phage fiber. Figure 1B–D illustrates the three

types of fibers constructed: silverized fibers comprising genetically engineered E3 phage (E3–Ag, Fig. 1B), silverized fibers comprising wildtype M13 phage (M13–Ag, Fig. 1C), and silverized composite E3 phage-coated Kevlar fibers (Kevlar–E3–Ag, Fig. 1D). These phage fibers and coatings were then exposed to various microbial challenges described below using *Escherichia coli* (*E. coli*) and *Staphylococcus epidermidis* (*S. epidermidis*) as representative Gram-negative and Gram-positive species. Additionally, fibers were subjected to bacteria cultured from human secretions to reflect challenges associated with antibacterial textile or wound dressing applications.

2. Results and Discussion

We employed scanning electron microscopy (SEM) and energy dispersive spectroscopy (EDS) to characterize the relative degree of silverization on E3 (modified) and M13 (unmodified) phage fibers (Fig. 2A and B). Successful genetic manipulation is evidenced by the comparative heights of the Ag$_{L\alpha}$ peaks from E3–Ag and M13–Ag in the EDS analyses (Fig. 2C) with the higher peak indicating greater silver loading on E3–Ag fibers. Inductively coupled plasma atomic emission spectroscopy (ICP–AES) was employed to determine the silver mass per length on these fibers, indicating $0.61 \pm 0.072\ \mu g\ cm^{-1}$ for E3–Ag fibers as compared to only $0.19 \pm 0.024\ \mu g\ cm^{-1}$ for M13–Ag (Fig. 2D). Amplification of the negative surface charge of phage fiber via E3 genetic modification thus results in approximately three times the degree of silver loading.

The bactericidal effects of this increased silver loading were visualized by fluorescence-based live-dead staining. Fibers were exposed to *E. coli* cells stained prior to indicate either intact (green) or lysed (red) cell membranes; red stain thus indicates dead bacteria. After 2 h, the fibers and cells were examined under fluorescent filters to determine live–dead cell counts. During this time span, E3–Ag fibers killed virtually all *E. coli* bacteria (99% ± 0.98%) within a 300 μm distance from the fiber (Fig. 3A and C). However, M13–Ag fibers proved less potent, displaying only a 74% ± 14% bacterial inhibition ratio within the same perimeter (Fig. 3B and D).

Bactericidal activity of these fibers was also characterized for longer time spans in modified disk diffusion (Kirby–Bauer) tests. Here, fibers were incubated in bacteria cultures overnight under agar and inspected for colony growth. Bactericidal activity was evidenced by zones of inhibition (ZoIs) where colony growth was prevented around the fibers. Unsilverized phage fibers (M13 or E3 fibers) did not exhibit any antibacterial ZoIs (Fig. 4A and B), confirming that these phage fibers are not inherently antibacterial to the *E. coli* or *S. epidermidis* (not shown) strains considered herein. (This result is expected, in that these M13 phages are capable of nonlytic infection in only specific strains of *E. coli* containing the F-pilus, and infection by phage is distinct from adhesion to phage-based fibers.) In contrast, silver ion leaching from the silverized
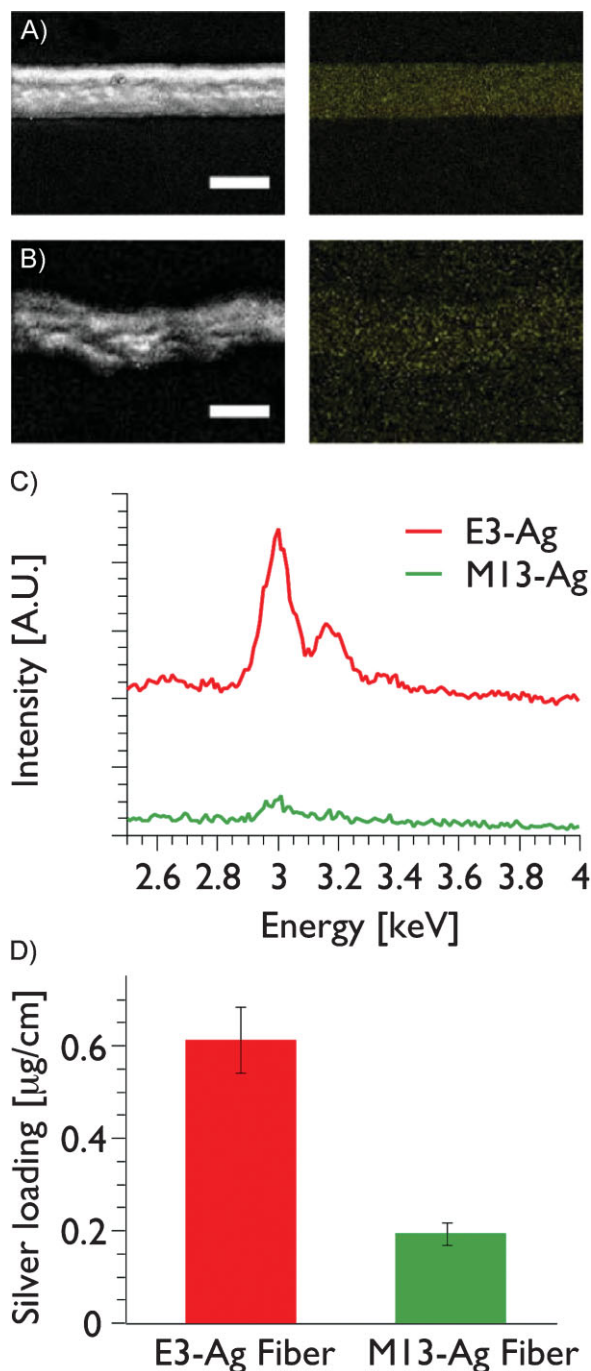
Materials
Views
www.MaterialsViews.com

ADVANCED
FUNCTIONAL
MATERIALS
www.afm-journal.de

FULL PAPER

Figure 2. Comparison of degree of silverization on E3 (engineered) and M13 (wildtype) phage fibers. A) SEM (left) backscattering and EDS maps (right) indicate dense, uniform adhesion of Ag particles to E3 phage fibers, whereas images in (B) demonstrate lower binding affinity to the unmodified M13 phage fibers. C) EDS analysis of $Ag_{L\alpha}$ peaks (arbitrary units) and D) ICP–AES quantify increased degree of silverization on engineered E3 phage fibers. EDS spectra shifted vertically for clarity. Scale bar = 50 μm.

Figure 3. Bactericidal activity (in contrast to growth inhibition) of phage fibers is confirmed via live–dead staining of *E. coli*. Bacteria within a 300 μm distance from the fiber edge of the A) E3–Ag fiber and B) M13–Ag fiber are shown after incubating fibers in a culture of *E. coli* ($OD_{600} = 0.1$) under agar at 37 °C for 120 min. Live bacteria are indicated as green, and dead as red (examples indicated by arrows). Fiber edge is demarcated by yellow dashed lines. Scale bar = 100 μm. C) Live–dead cell counts for replicate experiments confirm a significantly higher percentage of dead cells near the E3–Ag phage fibers. *Statistically significant by student *t*-test, *n* = 3 per phage fiber, *p* = 0.04.

fibers prevented colony growth, creating a zone of inhibition around the fibers (Fig. 4C–F). ZoI sizes (measured perpendicularly from the center of the fiber to the first sign of bacteria colony growth) are qualitatively larger for E3–Ag fibers (Fig. 4C and E) as
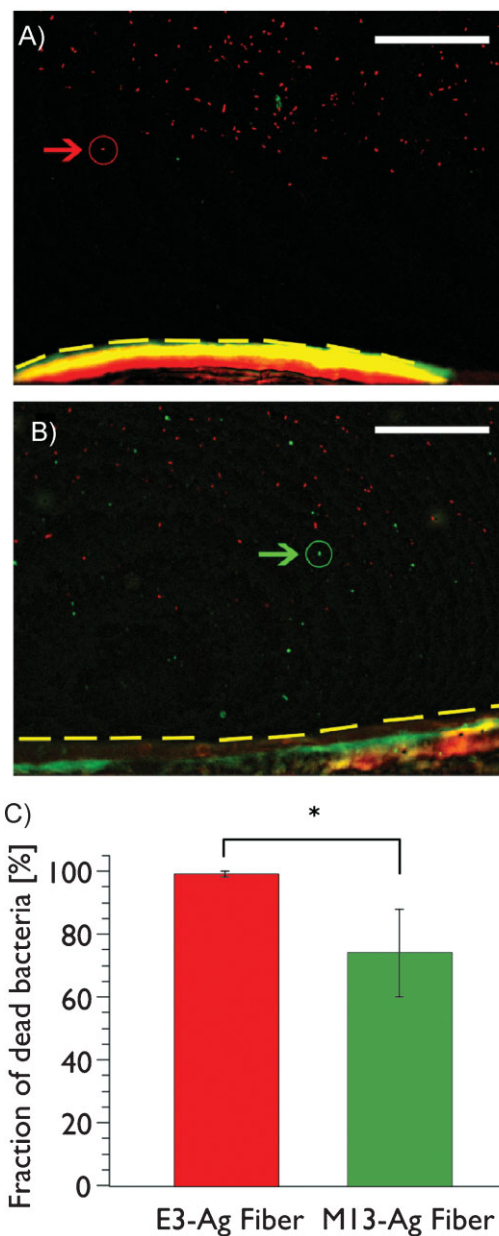
compared to M13–Ag fibers (Fig. 4D and F). It is commonly accepted that quantitative conclusions cannot be drawn from these modified disk diffusion tests (e.g., mathematical relations between ZoI size and silver loading on or ion diffusivity from the M13–Ag and E3–Ag fibers), as environmental and medium conditions are
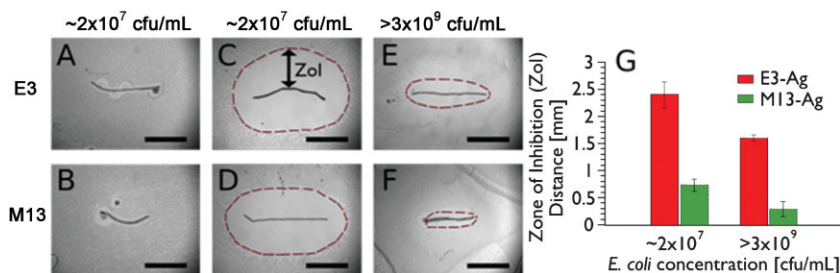
FULL PAPER

Figure 4. Antibacterial activity is characterized by ZoIs of *E. coli* growth (red dashed line) in modified disk diffusion tests. Unsilverized fibers comprising A) E3 phage and B) M13 phage show no ZoIs, confirming that phage fibers are not inherently bactericidal. C–F) For both phage fiber types, ZoIs are reduced at higher bacteria concentrations. However, for a given bacteria concentration, ZoIs are larger for the genetically engineered E3–Ag phage fibers as compared to wildtype M13–Ag phage fibers. G) Summary of these trends among replicate experiments ($n = 4$). Scale bar = 2 mm.

difficult to standardize in replicate bacteria incubations and the silver particles may be inhomogeneously distributed on the fibers.[23] However, the overall larger ZoIs surrounding E3–Ag fibers indicate stronger antibacterial potency in the genetically engineered fibers. This comparison corroborates the live–dead stain findings relevant to the earlier time points of bacteria–fiber interactions.

Exposing the fibers to higher bacteria concentrations ($>10^9$ cfu mL^{-1}, cfu = colony forming units) resulted in decreased ZoI sizes, as demonstrated in comparing Fig. 4E and C for E3–Ag fibers (and Fig. 4F and D for M13–Ag fibers). Despite 20 h of incubation in extremely high-density bacteria cultures, the silverized fibers were still able to maintain minimal ZoIs. The disk diffusion trends over replicate experiments ($n = 4$ for each condition) are summarized graphically in Fig. 4G. Modified disk diffusion tests with *S. epidermidis* cultures gave similar results in the comparison of M13–Ag and E3–Ag fibers (data not shown), supporting our expectation that silverized fibers are equally effective against these Gram-positive and Gram-negative species.

To simulate a more realistic microbial challenge demanded of fibers incorporated within antimicrobial textiles, E3–Ag and M13–Ag fibers were immersed in bacteria cultured from perspiration swabbed from the human axilla (underarm) for 2 h at 37 °C. Fibers were then incubated under agar overnight at 37 °C. E3–Ag fibers remained uncontaminated by this challenge (Fig. 5A), but adhesion of viable bacteria and subsequent colony growth was observed on M13–Ag fibers (Fig. 5B). This demonstrates the capacity of E3–Ag phage fibers to resist adhesion of viable bacteria in challenges relevant for wearable applications that require minimal risk of bacterial infection or associated odor production.

Upon the successful construction of biocidal phage fibers, we considered whether modification of this phage processing could confer antimicrobial functionality to a mechanically robust base fiber as a coating. As a proof of practical application, we chose to cover individual Kevlar fibers with our genetically engineered E3 phage and silverize the composite fiber. Here, we dipped Kevlar fibers into a highly concentrated E3 phage solution and then transferred them to the glutaraldehyde solution for crosslinking. Silverization was performed as with the phage fibers. These composite Kevlar–E3–Ag fibers have potential use in preventing odor-based detection in protective clothing, as well as reducing the

risk of infection to surface skin wounds exposed to soiled clothing. SEM and EDS of surface chemical composition confirmed successful silverization of the Kevlar fibers (Fig. 6A–C). Again, modified disk diffusion tests were used to characterize the bactericidal capability of the coatings. Under moderate bacteria concentrations ($\sim10^7$ cfu mL^{-1}), the Kevlar–E3–Ag exhibits more limited antibacterial potency, exhibiting smaller ZoIs (Fig. 6E–F) than the pure phage fibers in Figure 4. This reduced potency is attributable chiefly to less E3 phage—and thus less silver loading—in the composite E3–Ag-coated Kevlar fiber compared to a pure E3–Ag phage fiber. The E3–Ag coating, of $\sim$3–4 µm thickness surrounding the Kevlar fiber core of 9.3 µm diameter, decreases the functionalizable E3 volume as compared to the pure E3–Ag phage fibers of $\sim$40–100 µm diameter. Using our ICP–AES measurements of Ag content for this glutaraldeyhyde-crosslinked E3–Ag and these average fiber diameters and coating thickness, we estimate silver loading to be 0.10 µg cm^{-1} of composite fiber. This sixfold reduction in silver loading as compared to the pure E3–Ag fibers (0.61 µg cm^{-1}) resulted, as expected, in smaller ZoIs under comparable bacteria challenges.

Although these phage fibers and coatings perform as viable biocides, this method still presents certain limitations from a
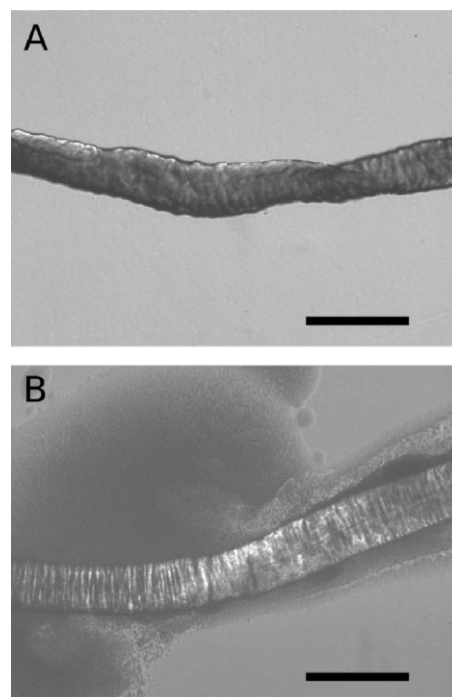

Figure 5. Adhesion of viable bacteria from normal human axilla (underarm) perspiration to phage fibers. Phage fibers comprising A) E3–Ag and B) M13–Ag were incubated in a culture of bacteria present in normal human perspiration (OD$_{540}$ = 0.04) for 2 h at 37 °C, then extracted and incubated under agar for 20 h at 37 °C. Colony growth was observed on the M13–Ag fibers, but not on E3–Ag fibers. Scale bar = 200 µm.
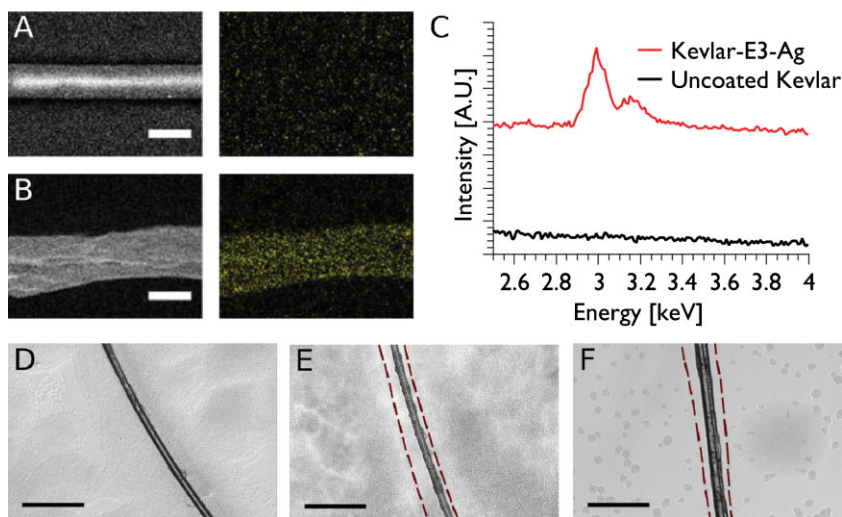
Materials
Views
www.MaterialsViews.com

ADVANCED
FUNCTIONAL
MATERIALS
www.afm-journal.de

FULL PAPER

Figure 6. Relative degrees of silverization on A) unmodified Kevlar and B) Kevlar coated with crosslinked E3 phage are characterized in SEM/EDS maps. Scale bar = 10 μm. C) Corresponding EDS spectra of E3–Ag-phage-coated Kevlar and unmodified Kevlar, characterized via $Ag_{L\alpha}$ peaks (arbitrary units). Spectra shifted vertically for clarity. Modified disk diffusion tests conducted on D) unmodified Kevlar, E) Kevlar–E3–Ag with *E. coli*, and F) Kevlar–E3–Ag with *S. epidermidis* indicate clear ZoIs (red dashed lines) in bacteria growth around only the phage-coated fibers. Scale bar = 100 μm.

3. Conclusions

In summary, we have successfully synthesized phage-based fibers that exhibit bactericidal activity against *E. coli*, *S. epidermidis*, and perspiration subcultures when functionalized with silver. Our results show that genetic engineering of the phage facilitates significant silverization (>600 ng cm^{-1} of fiber) and, correspondingly, strong antimicrobial effects. Examining bacteria cells under short time scales demonstrates the rapid bactericidal action of silver ions; bacterial cells within 300 μm of the fiber are killed within a 2 h exposure. Even under continued 20 h contact with bacteria concentrations as high as 10^9 cfu mL^{-1}, these silverized phage fibers are capable of inhibiting cell growth in the immediate vicinity, as demonstrated by the modified Kirby–Bauer tests of ZoI. This genetically engineered fiber also inhibits bacterial attachment and growth after undergoing a 2 h immersion in bacteria cultured from human perspiration, under challenges relevant to antimicrobial textile applications. Silver-functionalized, phage-coated Kevlar also displayed bactericidal activity, though to an extent reduced by the lower volume of the silverized phage as compared to pure phage fibers. Potential applications of these fibers and coatings include medical applications such as wound dressings, military applications to diminish armor odor, as well as commercial textiles such as athleticwear. Despite some upscaling limitations, the relatively facile and low-toxicity processing of these fibers presents certain advantages over other synthetic polymer-based biocidal textiles. Moreover, the successful integration of antimicrobial functionality within a biological scaffold shows promise for further genetic engineering toward the design of multifunctional fibers.

practical standpoint; these challenges are common to other antiseptic fiber technologies. Large quantities of phage fibers are difficult to manufacture at the research scale due to the high concentration of phage required (10^{15}–10^{16} pfu mL^{-1}, pfu = plaque forming units). Given the large volumes of bacteria required to yield such concentrations, large-scale synthesis of phage fibers would require a continuous bioreactor, as is used in industrial-scale phage production. Also, controllable release and distribution of silver particles would be a desirable feature to integrate into this design. However, in addition to the future prospect of multifunctionality, these phage fibers already demonstrate several advantages over alternate current fiber production techniques. First, the silver leaching results in relatively rapid bactericidal action (<2 h exposure, as evidenced by live–dead stains), which is beneficial over other fiber platforms that require prolonged hours of contact before cell death occurs. Second, phage fiber processing can be performed in ambient conditions, unlike many polymerization methods that demand high temperatures and inert atmospheres. Third, the extrusion, crosslinking, and silverization can be completed in less than an hour for continuous fibers of tens of centimeters in length, whereas chemical processing times can sometimes span days.[24,25] Thus, the relative ease of wet-spinning and electroless plating of these Ag phage fiber processing presents several advantages over synthetic antimicrobial polymer fiber platforms, considering the potency and efficacy of the imparted antimicrobial functionality. Further, this material platform offers the potential to combine multifunctional antimicrobial strategies (e.g., controlled release of expressed functional groups) and distinct functionalities (e.g., electrical conductivity) via further genetic manipulation or post-processing of E3 phage fibers.

4. Experimental

Fiber Preparation and Silverization: Highly concentrated phage solution (10^{15}–10^{16} pfu mL^{-1} in Milli-Q water) was extruded vertically through a 33-gauge needle into an 8 vol% glutaraldehyde solution (Sigma–Aldrich) by a syringe pump, producing approximately 2–3 cm per microliter of phage suspension. Fibers were incubated in glutaraldehyde solution for 20 min and then rinsed in Milli-Q water. Using forceps, fibers were then individually transferred to a bath of 5 mM silver acetate (Sigma–Aldrich) and incubated for 30 s. Subsequently, fibers were transferred to a bath of 5 mM sodium borohydride (EMD Chemicals, Inc.) and incubated for another 30 s before being rinsed with Milli-Q water. Finally, the fibers were extracted and dried in air.

Microscopy and Spectroscopy: Micrographs and fluorescent microscopy images were obtained with an optical microscope (Olympus IX51). SEM and EDS maps were obtained and analyzed with a LEO 438VP SEM operated at 20 kV with an electron-backscattering detector. E3–Ag and M13–Ag fibers, each approximately 10 cm in length, were dissolved in nitric acid, and the solution was analyzed with an ICP–AES (Horiba Jobin Yvon Activa) to obtain silver concentrations.

Bacterial Culture: *E. coli* (ATCC 700728) and *S. epidermidis* (ATCC 14990) were grown at 37 °C in a Luria–Bertani (LB) medium and diluted to

the desired concentrations as quantified by optical density measurements at wavelengths of 600 and 540 nm for *E. coli* and *S. epidermidis*, respectively.

Live–Dead Staining: *E. coli* (2×10^7 cfu mL^{-1}) were stained using the LIVE/DEAD BacLight Bacterial Viability Kit (Molecular Probes, L13152). Fibers approximately 3–4 cm in length were incubated in 15 μL of this *E. coli* culture under agar for 2 h at 25 °C in the dark. Cells were then visualized via fluorescence microscopy (Olympus IX51); cell counts were performed using ImageJ software.

Modified Disk Diffusion (Kirby-Bauer) Tests: Fibers approximately 3–4 cm in length were incubated in 15 μL of either *E. coli* or *S. epidermidis* cultures under agar for 20 h at 37 °C. Fibers were challenged with both low (~10^7 cfu mL^{-1}) and high (>10^9 cfu mL^{-1}) densities of bacteria culture. ZoI distances were measured from the micrographs using ImageJ software; distances were taken perpendicularly from the center of the fiber to the first visible bacterial colony.

Human Perspiration Challenge: Perspiration was swabbed from the axilla (underarm) of a normal healthy human and streaked onto a plate of LB agar, which was then incubated overnight at 37 °C. E3–Ag and M13–Ag fibers about 13 mm in length were soaked in a 250 μL culture of perspiration bacteria (concentration estimated to be ~10^7 cfu mL^{-1} based on growth time and probability of culturing mostly *S. epidermidis* cells) for 2 h. Fibers were then extracted with forceps and incubated under agar for 20 h at 37 °C.

Preparation of Virus-Based Kevlar Coating: Kevlar strands were dipped into a pool of highly concentrated phage solution (10^{15}–10^{16} pfu mL^{-1} in Milli-Q water) and drawn out with forceps. The coated Kevlar was immersed in 8 vol% glutaraldehyde solution and then silverized with same method described above for the phage fibers.

[1] G. Sykes, *Disinfection and Sterilization*, Van Nostrand, Princeton, NJ **1958**.

[2] S. L. Percival, P. G. Bowler, D. Russell, *J. Hosp. Infect.* **2005**, *60*, 1.

[3] M. J. Brady, C. M. Lisay, A. V. Yurkovetskiy, S. P. Sawan, *Am. J. Infect. Control* **2003**, *31*, 208.

[4] M. A. Hollinger, *Crit. Rev. Toxicol.* **1996**, *26*, 255.

[5] M. Kawashita, S. Tsuneyama, F. Miyaji, T. Kokubo, H. Kozuka, K. Yamamoto, *Biomaterials* **2000**, *21*, 393.

[6] I. Sondi, B. Salopek-Sondi, *J. Colloid Interface Sci.* **2004**, *275*, 177.

[7] D. Lee, R. E. Cohen, M. F. Rubner, *Langmuir* **2005**, *21*, 9651.

[8] D. S. Katti, K. W. Robinson, F. K. Ko, C. T. Laurencin, *J. Biomed. Mater. Res. Part B* **2004**, *70B*, 286.

[9] V. Acharya, C. R. Prabha, C. N. Murthy, *J. Polym. Mater.* **2003**, *20*, 83.

[10] A. Melaiye, Z. H. Sun, K. Hindi, A. Milsted, D. Ely, D. H. Reneker, C. A. Tessier, W. J. Youngs, *J. Am. Chem. Soc.* **2005**, *127*, 2285.

[11] W. K. Son, J. H. Youk, T. S. Lee, W. H. Park, *Macromol. Rapid Commun.* **2004**, *25*, 1632.

[12] S. H. Hsieh, Z. K. Huang, Z. Z. Huang, Z. S. Tseng, *J. Appl. Polym. Sci.* **2004**, *94*, 1999.

[13] T. Mikolajczyk, D. Wolowska-Czapnik, M. Bogun, *J. Appl. Polym. Sci.* **2008**, *107*, 1670.

[14] S. H. Wang, W. S. Hou, L. Q. Wei, H. S. Jia, X. G. Liu, B. S. Xu, *Surf. Coat. Technol.* **2007**, *202*, 460.

[15] J. S. Patel, S. V. Patel, N. P. Talpada, H. A. Patel, *Angew. Makromol. Chem.* **1999**, *271*, 24.

[16] E. R. Kenawy, F. I. Abdel-Hay, A. El-Raheem, R. El-Shanshoury, M. H. El-Newehy, *J. Controlled Release* **1998**, *50*, 145.

[17] E. R. Kenawy, F. I. Abdel-Hay, A. A. El-Magd, Y. Mahmoud, *J. Appl. Polym. Sci.* **2006**, *99*, 2428.

[18] S. Z. Tan, G. J. Li, J. R. Shen, Y. Liu, M. H. Zong, *J. Appl. Polym. Sci.* **2000**, *77*, 1869.

[19] C. Y. Chiang, C. M. Mello, J. J. Gu, E. Silva, K. J. Van Vliet, A. M. Belcher, *Adv. Mater.* **2007**, *19*, 826.

[20] Y. Huang, C. Y. Chiang, S. K. Lee, Y. Gao, E. L. Hu, J. De Yoreo, A. M. Belcher, *Nano Lett.* **2005**, *5*, 1429.

[21] C. B. Mao, D. J. Solis, B. D. Reiss, S. T. Kottmann, R. Y. Sweeney, A. Hayhurst, G. Georgiou, B. Iverson, A. M. Belcher, *Science* **2004**, *303*, 213.

[22] K. T. Nam, Y. J. Lee, E. M. Krauland, S. T. Kottmann, A. M. Belcher, *ACS Nano* **2008**, *2*, 1480.

[23] C. H. Nightingale, T. Murakawa, Paul, G. Ambrose, *Antimicrobial Pharmacodynamics in Theory and Clinical Practice*, Informa Health Care, New York, NY **2002**.

[24] C. Z. S. Chen, N. C. Beck-Tan, P. Dhurjati, T. K. van Dyk, R. A. LaRossa, S. L. Cooper, *Biomacromolecules* **2000**, *1*, 473.

[25] A. Popa, C. M. Davidescu, R. Trif, G. Ilia, S. Iliescu, G. Dehelean, *React. Funct. Polym.* **2003**, *55*, 151.